Formation Conditions of Titan's and Enceladus's Building Blocks in Saturn's Circumplanetary Disk

Sarah E. Anderson, Olivier Mousis, Thomas Ronnet

The Planetary Science Journal, 2:50 (8pp), 2021 April https://doi.org/10.3847/PSJ/abe0ba

Formation Conditions of Titan's and Enceladus's Building Blocks in Saturn's Circumplanetary Disk

Sarah E. Anderson[1,2], Olivier Mousis[1], and Thomas Ronnet[3]
[1] Aix Marseille University, CNRS, CNES, LAM, Marseille, France; sarah.anderson@univ-fcomte.fr
[2] University Bourgogne Franche-Comté, OSU THETA, Besançon, France
[3] Lund Observatory, Department of Astronomy and Theoretical Physics, Lund University, Box 43, SE-22100, Lund, Sweden
Received 2020 June 22; revised 2021 January 21; accepted 2021 January 26; published 2021 March 12

Abstract

The building blocks of Titan and Enceladus are believed to have formed in a late-stage circumplanetary disk (CPD) around Saturn. Evaluating the evolution of the abundances of volatile species in this disk as a function of the migration, growth, and evaporation of icy grains is then of primary importance to assess the origin of the material that eventually formed these two moons. Here we use a simple prescription of Saturn's CPD in which the location of the centrifugal radius is varied, to investigate the time evolution of the icelines of water ice, ammonia hydrate, methane clathrate, carbon monoxide, and dinitrogen pure condensates. To match their compositional data, the building blocks of both moons would have had to form in a region of the CPD situated between the icelines of carbon monoxide and dinitrogen at their outer limit, and the iceline of methane clathrate as their inner limit. We find that a source of dust at the location of centrifugal radius does not guarantee the replenishment of the disk in the volatiles assumed to be primordial in Titan and Enceladus. Only simulations assuming a centrifugal radius in the range 66–100 Saturnian radii allow for the formation and growth of solids with compositions consistent with those measured in Enceladus and Titan. The species are then able to evolve in solid forms in the system for longer periods of time, even reaching an equilibrium, thus favoring the formation of Titan and Enceladus's building blocks in this region of the disk.

Unified Astronomy Thesaurus concepts: Saturnian satellites (1427); Natural satellite formation (1425)

1. Introduction

The exploration of Saturn's satellite system by the Cassini–Huygens spacecraft has revealed several puzzling features regarding the compositions of the moons Titan and Enceladus, prompting the revision of their formation models. While the Huygens probe's descent to Titan's surface confirmed that the atmosphere is dominated by N_2 and CH_4, with a very low CO:CH_4 ratio ($\sim 10^{-3}$) as previously found by Voyager and ground-based observations (Gautier & Raulin 1997), it also revealed a significant depletion of the primordial noble gases. The only definitively observed primordial noble gas detected by the Gas Chromatograph Mass Spectrometer (GCMS) aboard the Huygens probe was ^{36}Ar, with a $^{36}Ar/^{14}N$ ratio lower than the solar value by more than five orders of magnitude (Niemann et al. 2005, 2010). The other primordial noble gases Kr and Xe (and ^{38}Ar) were not detected by the GCMS instrument down to upper limits of 10^{-8} relative to nitrogen (Niemann et al. 2005). These absences of detections are puzzling because noble gases are notable in the atmospheres of telluric planets (Pepin 1992; Wieler 2002), as well as in the atmosphere of Jupiter (Owen et al. 1999; Mousis et al. 2019). The depletion in CO is also a strong constraint on Titan's composition since it is believed to have been more abundant than CH_4 in the protosolar nebula (PSN) (Mumma & Charnley 2011; Bockelée-Morvan et al. 2004; Bockelée-Morvan & Biver 2017). Since CO shares a similar volatility with N_2, its very low abundance in Titan's atmosphere is consistent with the strongly supported interpretation that the observed N_2 is probably not primordial and would result from photolysis, shock chemistry, or thermal decomposition of primordial NH_3 (Atreya et al. 1978; McKay et al. 1988; Matson et al. 2007; Sekine et al. 2011; Mandt et al. 2014; Miller et al. 2019). In addition, the flyby of Enceladus's south pole by the Cassini spacecraft allowed the measurement of the composition of its plumes by the Ion and Neutral Mass Spectrometer (INMS), unveiling a 96%–99% concentration of H_2O, along with small amounts of CO_2 (0.3%–0.8%), CH_4 (0.1%–0.3%), NH_3 (0.4%–1.3%), and H_2 (0.4%–1.4%) (Waite et al. 2017). Also, ^{36}Ar, CO, and N_2 were not detected by the INMS instrument in open-source mode, strengthening the argument that the building blocks of Enceladus may have formed devoid of these three molecules.

Together, the measurements of Titan's and Enceladus's compositions suggest that they could have been assembled from similar building blocks. This scenario has been developed by Mousis et al. (2009a, 2009b), who proposed that both moons formed from building blocks initially produced in the PSN prior to having been partially devolatilized in a temperature range between the formation temperatures of CO and N_2 pure condensates and the crystallization temperature of CH_4 clathrate in Saturn's circumplanetary disk (CPD). By doing so, Titan's and Enceladus's building blocks would have been devoid of CO and N_2, while still keeping the entrapped CH_4 to match the observed compositions. However, these two studies did not investigate the transport (gas diffusion and drift of solid particles) of key volatiles around the locations of their respective icelines.

An iceline is defined as the radius at which the disk temperature is equal to the sublimation or condensation temperature of water ice (or any species of interest) in the PSN and CPDs. Inside the iceline, ice sublimates. Outside, ice

remains stable, though the motion of particles within the disk would allow for solids to exist in front of this line as well as some vapors to exist beyond. Thus, the icelines induce the creation of peaks of abundances of volatile species in disks (Ali-Dib et al. 2014; Mousis et al. 2019; Aguichine et al. 2020). Tracking the abundances of volatiles in both solid and vapor states around their respective icelines should then provide tighter constraints than previous works on the locations at which the building blocks of Titan and Enceladus formed, assuming that their volatile content is essentially primordial.

Here we aim to explore the time evolution of the icelines of H_2O ice, NH_3 hydrate, CH_4 clathrate, CO, and N_2 pure condensates, i.e., the key volatiles needed to explain Titan's and Enceladus's observed compositions, within Saturn's CPD and derive their impact on the formation conditions of the two satellites' building blocks. Our approach is based on a simple prescription of a CPD model (Canup & Ward 2002; Sasaki et al. 2010) and follows the dynamic radial evolution of icy dust and gases as they cross over the various icelines, estimating growth, fragmentation, and condensation as they drift within the disk. The simulation also follows the evolution of the different vapors as they condense on the grain surfaces or become enriched if icy grains evaporate.

An important parameter in our simulations is the location of the centrifugal radius R_c, which corresponds to the point where the angular momentum of the incoming gas is in balance with the gravitational potential of Saturn. It is also the injection point of the solid material entering the CPD from the PSN (Canup & Ward 2002; Sasaki et al. 2010), and its value is overall poorly constrained in CPDs. For instance, to account for the orbital distribution of the Galilean satellites, R_c has been estimated to be in the ~20–30 $R_{\rm Jup}$ range in Jupiter's CPD (Ruskol 1982). This range could be somewhat larger if some inward type I migration of satellite embryos is taken into account, perhaps R_c ~ 35–40 $R_{\rm Jup}$ (Canup & Ward 2002). In the case of Saturn's CPD, Sasaki et al. (2010) have opted to set $R_c = 30\,R_{\rm Sat}$ ($R_{\rm Sat}$ is the radius of Saturn), by similarity with previous studies of the Jovian CPD, while Machida (2009) finds $R_c = 66\,R_{\rm Sat}$, by taking into account the specificity of the disk (lower mass of the planet and larger Hill radius). On the other hand, recent simulations of gas accretion onto a CPD show that the material infalling toward the subdisk could be distributed out to much larger distances, of the order of ~100 R_p (Szulágyi 2017). Here, we investigate the influence of the variation of R_c's location in the formation region of the satellites' building blocks. This allows us to show that the abundance of solid material within this disk depends strongly on the radial distance of its injection point.

Section 2 is dedicated to the description of the disk and transport models. Section 3 presents the results of several computations with different initial conditions for the delivery of particles from the CPD, namely different positions of R_c. Conclusions are presented in Section 4.

2. Model

2.1. Gas-starved Accretion Disk

We consider a circum-Saturnian accretion disk with an inflow of material from the surrounding PSN based on the approaches of Canup & Ward (2002) and Sasaki et al. (2010). It is limited by the outer radius $R_d = 200\,R_{\rm Sat}$ by processes such as solar torques or through collisions with shocked regions. The CPD is fed through its upper layers from its inner edge up to the centrifugal radius R_c by gas and gas-coupled solids inflowing from the PSN. In the following, we start with the assumption that $R_c = 30\,R_{\rm Sat}$ (Canup & Ward 2002), and also investigate several cases at different radii within the CPD (see Section 3). In this 1D model, for each point of the radius r, we have an integrated surface density Σ that describes the integrated density over the vertical slice of the disk. The quantities that interest us are the surface density of the dust Σ_d and the surface density of the vapor Σ_v. These will be compared to the surface density of the PSN gas, Σ_g. Here, "dust" refers to icy grains.

The surface density of the disk gas is given by (Canup & Ward 2002)

$$\Sigma_g \simeq \frac{4F_p}{15\pi\nu}\lambda(r), \tag{1}$$

where F_p is the total infall rate and ν is the turbulent viscosity of the disk gas. The turbulent viscosity of the CPD is defined via $\nu = \alpha C_s^2/\Omega_{\rm K}$ (Shakura & Sunyaev 1973), where α (set to 10^{-3}) is the viscosity parameter. $\Omega_K = \sqrt{GM_{\rm Sat}/r^3}$ is the Keplerian frequency with G defined as the gravitational constant and $M_{\rm Sat}$ is the mass of Saturn. C_s is the isothermal sound speed given by $C_s = \sqrt{kT/\mu m_p}$, where k is the Boltzmann constant, μ the mean molecular weight, and m_p the proton mass. The coefficient $\lambda(r)$ is set equal to

$$\begin{aligned} \lambda(r) &= \frac{5}{4} - \sqrt{\frac{R_c}{R_d}} - \frac{1}{4}\left(\frac{r}{R_c}\right)^2 \text{ for } r < R_c, \\ \text{and } \lambda(r) &= \sqrt{\frac{R_c}{r}} - \sqrt{\frac{R_c}{R_d}} \text{ for } r \geqslant R_c. \end{aligned} \tag{2}$$

In the steady accretion state, the total infall rate is regulated by a parameter $\tau_G = M_{\rm Sat}/(dM/dt)$, where dM/dt is the inflow rate, so that $F_{p,0} = M_{\rm Sat}/\tau_G$. We adopt $\tau_G = 5 \times 10^6$ yr for Saturn (Sasaki et al. 2010). The total infall rate follows an exponential decay via $F_p = F_{p,0}\exp(-t/\tau_{\rm Dep})$, with the timescale of CPD depletion $\tau_{\rm Dep}$ set to 3×10^6 yr (Canup & Ward 2006; Sasaki et al. 2010).

The CPD is heated by luminosity from the central planet, viscous dissipation, and energy dissipation associated with the difference between the freefall energy of the incoming gas and that of a Keplerian orbit. Assuming that viscous dissipation is dominant, the photosurface temperature of the CPD (T_d) is determined by a balance between viscous heating and blackbody radiation from the photosurface (Canup & Ward 2002; Sasaki et al. 2010):

$$\sigma_{sb}T_d^4 \simeq \frac{9}{8}\Omega_K^2\nu\Sigma_g = \frac{3\Omega_K^2}{10\pi}F_p\,\lambda(r). \tag{3}$$

The disk temperature profile at $t = 0$ can then be given as follows:

$$T_{d,0}^4 = \frac{3\Omega_K^2}{10\pi\sigma_{sb}}F_{p,0}\,\lambda(r). \tag{4}$$

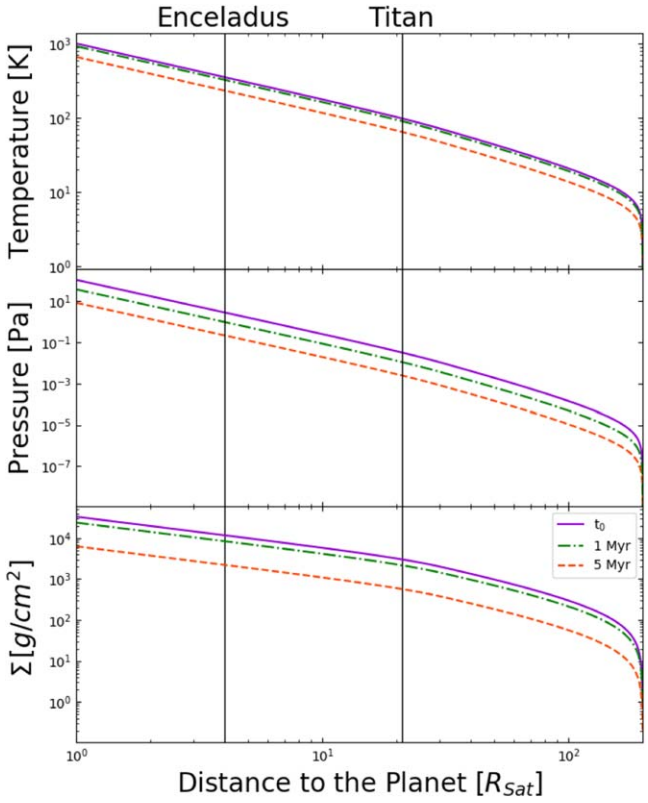

Figure 1. Disk steady-state pressure, temperature, and gas surface density for the gas-starved accretion disk model of Saturn at $t = 0$ (solid lines), $t = 10^6$ yr (dotted–dashed lines), and $t = 5 \times 10^6$ yr (dashed lines) for $R_c = 30\ R_{\rm Sat}$. The evolution of these quantities is very slow in the CPD and can even be seen as stationary over short timescales. The present day locations of Enceladus and Titan are shown for reference.

Using this expression, the disk temperature can be written as a function of time:

$$T_d \simeq T_{d,0} \exp\left(\frac{-t}{4\tau_{\rm dep}}\right). \tag{5}$$

The inflow rate is also constrained by the requirement that temperatures be low enough for pure condensates to remain stable in the outer regions of Saturn's CPD, a requirement that this model fulfills without alteration, showing similar values as Canup & Ward (2002) for the Jupiter disk. Figure 1 presents the thermodynamic properties of the CPD model used throughout this paper with $R_c = 30\ R_{\rm Sat}$.

2.2. Grain Size Evolution

The dust evolution model is derived from the approach of Birnstiel et al. (2012). The particles are evenly injected into the disk with a uniform size $a = 10^{-6}$ m. These micron-sized crystalline icy grains evolve in size and position through collisions, fragmentation, and radial drift due to gas drag. In our calculations, the size of grains increases before it reaches an equilibrium corresponding to the minimum value between fragmentation and radial drift.

Fragmentation occurs when the relative velocity of the dust grains due to turbulent motion exceeds the fragmentation velocity threshold u_f. We set the latter to $10\ {\rm m\ s^{-1}}$ (Birnstiel et al. 2012). The dust internal density is set to $\rho_s = 1\ {\rm g\ cm^{-3}}$. The size of the grains, limited by their fragmentation, is (Birnstiel et al. 2012)

$$a_{\rm frag} = 0.37 \frac{2\Sigma_g}{3\pi\rho_s\alpha} \frac{u_f^2}{c_s^2}. \tag{6}$$

In many cases, the grains drift inward too quickly for them to grow any larger. The size of these grains, limited by their drift, is given by

$$a_{\rm drift} = 0.55 \frac{2\Sigma_d}{\pi\rho_s} \frac{v_K^2}{c_s^2} \left| \frac{d\ln P}{d\ln r} \right|^{-1}, \tag{7}$$

where v_K is the Keplerian velocity, $P = c_s^2 \rho_g$ and $\rho_g = \Sigma_g / 2\pi H_g$ the pressure and gas density at midplane, with H_g the gas scale height. The prefactor $f_d = 0.55$ accounts for the shift of the representative size as compared to the maximum attainable size of the dust grains (Birnstiel et al. 2012).

2.3. Transport Model

We assume that all the species are simultaneously released into the disk, and that this mixture has the composition of the PSN, a mixture that radially diffuses and advects. Both species are initially in solid or gaseous forms, depending on where they are in the disk. Σ_i represents the surface density of species i we intend to study in either vaporous or solid form. We integrate the advection–diffusion equation using a forward Euler integration (Birnstiel et al. 2012):

$$\frac{\partial\Sigma_i}{\partial t} + \frac{1}{r}\frac{\partial}{\partial r}\left[r\left(\Sigma_i v_i - D_i \Sigma_g \frac{\partial}{\partial r}\left(\frac{\Sigma_i}{\Sigma_g}\right)\right)\right] + \dot{Q} = 0 \tag{8}$$

where v_i and D_i are the radial velocity and the diffusivity of species i respectively. $\dot{Q}$ corresponds to the source term of species i vapor released to the gas and is given by $\Sigma_{\rm ice}/\Delta t$ beyond the iceline, with Δt the time step of the simulation. The last values to calculate are the velocity of the dust v_d, the Stokes number St, the radial velocity of the gas, and the diffusivity (Birnstiel et al. 2012). v_d is given by

$$v_d = -\frac{2St}{1 + St^2}\eta v_K + \frac{1}{1 + St^2} v_g, \tag{9}$$

where v_g is the radial inward gas velocity given by $v_g = -3\nu/2r$, with ν the turbulent diffusivity of the gas described in Section 2.1, and $\eta = -(1/2)h_g^2 d\ln P/d\ln r$ is a measure of the pressure support of the disk, where $h_g \equiv H_g/r$ is the aspect ratio of the disk. In other words, the parameter η describes the deviation of the azimuthal velocity of the gas from the Keplerian value, $v_{\phi,g} = (1-\eta)v_K$. The Stokes number describes the aerodynamic properties of the particles and is determined as follows:

$$St = \frac{a\pi\rho_s}{2\Sigma_g}. \tag{10}$$

Finally, the diffusivity D of the vapor species is assumed to be that of the gas, $D_g = \nu$, and the diffusivity of the dust is given

Table 1
Parameters Adopted for Equations (See Section 2) Describing the Equilibrium Vapor Pressure Curves of Different Condensates

Species X	A	B	X/H_2
H_2O	−1750.286	7.2326	4.43×10^{-4}
NH_3	−2878.23	8.00205	4.05×10^{-5}
CH_4	−2161.81	11.1249	3.16×10^{-6}
CO	−411.24	5.2426	2.21×10^{-4}
N_2	−360.07	4.7459	4.05×10^{-5}

Note. Gas-phase abundances are provided as volume mixing ratios relative to H_2.

by

$$D_d = \frac{D_g}{1 + St^2}. \quad (11)$$

2.4. Source Term

The dust surface density decreases in the CPD until almost no particles are left over very short time frames (less than 10^4 yr). A disk that depletes at this rate would not be able to survive over the timescales necessary for satellite formation. Our observations on the sustainability of particles in Saturn's CPD agree with those of Ronnet et al. (2017). Their model for the motion of particles of different sizes evolving in the Jupiter system model found that small particles of the order of 10^{-6} m moved very rapidly in Jupiter's disk, often dispersing entirely in less than 500 yr. Particles over 10^{-1} m ablated in much less time, often entirely sublimating in less than 20 yr.

These simulations show that no disk could be sustainable at the rate of accretion we are seeing here. An additional source of solids needs to be added so that our solid particles could continue to exist over the timescales necessary for the formation of moons. To overcome this issue, we follow the prescription of Canup & Ward (2002) that injects solids directly into the disk at the centrifugal radius R_c. As gas and solids are delivered to the disk, the gas then sustains a quasi-steady state, while the surface density of the solids build up over time. While the gas component of the disk viscously spreads outward and onto the planet, the solids rapidly accumulate in the region where they are initially delivered, providing a mechanism for accreting large satellites in a limited region extending from the surface of the planet to the centrifugal radius R_c. This would also explain why we do not see large moons beyond this radius, despite the tidal stability of the region. The injection rate of solids $\dot{\Sigma}_{\rm solids}$ at the centrifugal radius R_c of the CPD is then (Canup & Ward 2002)

$$\dot{\Sigma}_{\rm solids} = \begin{cases} \frac{f \times F_p}{\pi R_c^2} & r < R_c \\ 0 & r > R_c \end{cases}, \quad (12)$$

where f is the solids-to-gas ratio in the region of regular satellites, here assumed to be $\sim 7.5 \times 10^{-4}$ (volume mixing ratio). This value corresponds to the sum of the gas-phase abundances of the species considered in our study (see Table 1).

3. Results

We place our work in the context of the satellite formation scenario proposed by Mousis et al. (2009a, 2009b), in which the building blocks of both Titan and Enceladus are assumed to be formed between the locations of the CH_4 clathrate iceline and the icelines of CO and N_2 pure condensates in Saturn's CPD. In this way, the satellites' building blocks are presumed to be devoid of primordial CO and N_2 while they retain the trapped CH_4, in agreement with Titan's and Enceladus's composition measurements.

In order to determine the positions of the icelines of H_2O ice, NH_3 hydrate, CH_4 clathrate, CO, and N_2 pure condensates, we compute the partial pressure of species i at each incremental radius. We then calculate the equilibrium pressure of the species based on the temperature at that radius and compare it to the partial pressure. Equilibrium pressure equations for H_2O, CO, and N_2 pure ices derive from Mousis et al. (2008) and are in the form $\log P = A/T + B$, where P and T are the partial pressure (bars) and the temperature (K) of the considered species, respectively. Equilibrium pressure equations for NH_3 hydrate and CH_4 clathrate derive from Hersant et al. (2004) and are also in the form $\ln P = A/T + B$. If the partial pressure of the species exceeds its equilibrium pressure at that radius, the species will be solid. Otherwise, it will sublimate. The gas-phase composition of Saturn's CPD is also assumed to be protosolar (Mousis et al. 2009a). The abundances of the different species are derived from the assumption that all O is distributed between H_2O and CO, all N is in the form of N_2 and NH_3, and C is only in the form of CO and CH_4, with a CH_4/CO ratio of 0.014 (Mousis et al. 2009a). Table 1 shows the parameters A and B derived from Hersant et al. (2004) and Mousis et al. (2008) and adopted for the different equilibrium curves, as well as the abundances of relevant species taken from Mousis et al. (2009a). In the following, we first investigate the evolution of solids within the CPD assuming the location of R_c is $30\,R_{\rm Sat}$, a value consistent with those estimated in Jupiter's CPD (Canup & Ward 2002), then we study the influence of placing this parameter at larger saturnocentric distances.

Each species is characterized by its own surface density in the CPD, in either gas or solid phase, whose value is derived from the disk's surface density and its individual abundance. At $t = 0$, the CPD model is filled with dust whose composition is determined from our initial ratios. Any species located closer to Saturn than its corresponding iceline is in the gaseous phase. Beyond their respective icelines, these species are in dust form with sizes of 10^{-6} m.

3.1. Evolution of Solids Assuming $R_c = 30\,R_{Sat}$

Figure 2 presents the quantity of dust in the system before any motion has occurred, giving us a visual representation of the location of icelines. At this epoch, the sublimation temperatures and iceline locations are 153.5 K and 12.0 $R_{\rm Sat}$ for H_2O, 96.5 K and 21.1 $R_{\rm Sat}$ for NH_3 hydrate, 53.4 K and 40.7 $R_{\rm Sat}$ for CH_4 clathrate, 22.4 K and 90.4 $R_{\rm Sat}$ for CO, and 20.3 K and 103.7 $R_{\rm Sat}$ for N_2 pure condensates.

As the disk cools with time, the icelines migrate inward toward Saturn. However, on the short timescales that we are interested in, the disk can be seen as stationary and the inward migration of the icelines ignored. If Titan and Enceladus mainly assembled from pebbles formed between the iceline of CH_4 clathrate and those of CO and N_2 pure condensates, as is investigated here, the very slow cooling of our CPD model implies that the two moons never formed at their current positions. While it is possible for us to adjust the parameters of the disk so as to fit this constraint, there is no firm indication

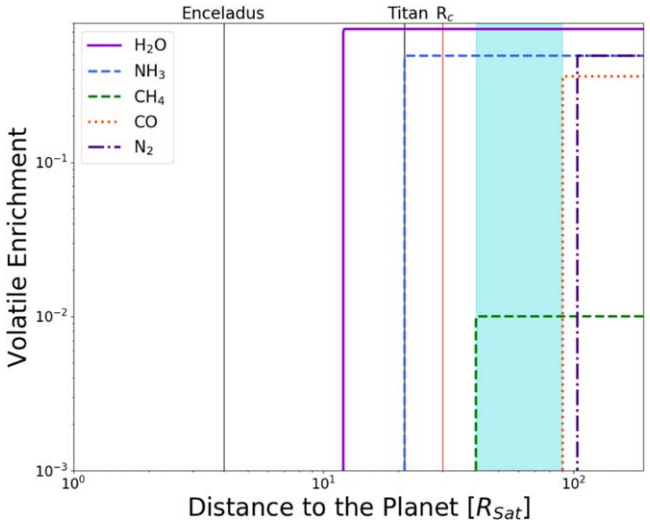

Figure 2. Initial enrichments in water, ammonia, methane, carbon monoxide, and nitrogen in solid forms, scaled to the elemental abundances, assumed to be protosolar (Lodders 2003). Current orbits of Enceladus and Titan, as well as the location of the centrifugal radius R_c, are shown for reference. The blue rectangle represents the ideal location for the formation of the building blocks of both moons in order to match their observed compositional data.

that the building blocks of the two bodies actually formed at their current location (see Section 4). They may have migrated in from further out in the disk, which is what we assume here.

As is evident in Figure 3, the dust surface density decreases over very short time frames in the CPD until none is left. In the case of H_2O, there is no gas or dust remaining in the disk after a mere 5×10^3 yr. This would seem to indicate that the moons would have formed very quickly, which is impossible based on even the most optimistic estimates, which require approximately 10^4 yr (Cilibrasi et al. 2018). As a result, we are forced to add a source term as established in Section 2.4, where a steady injection of solids is set at R_c. As we inject solids into the disk, most will continue to be sublimated as they are pulled through the different icelines during their inward drift. Figure 3 shows that, at a given epoch of the CPD evolution, the solid water abundance grows and then decreases radially because of the diffusion of vapor beyond the iceline. At any given location of R_c, the water abundance also increases and then decreases over time until it reaches a steady state. This state is reached after 3×10^3 yr. This creates a zone where the quantity of solid H_2O is stable for a long period of time.

Figure 4 depicts the evolution of H_2O, NH_3, CH_4, CO, and N_2 in solid phases as a function of the distance to Saturn in the CPD over 10^4 yr of disk evolution, with the injection of solids. Because the icelines of NH_3 and (to a lesser extent) of H_2O are closer to the location of the injection point of solids (R_c), these species keep significant solid abundances in the disk. CO, CH_4, and N_2, whose respective icelines are far beyond the position of R_c, are depleted before enough time has passed for any building blocks to form. Also, altering the solids-to-gas ratio has no effect on the lifetime of these solids because it has no influence on the location of injection. In this case, the building blocks of Titan and Enceladus cannot incorporate significant amounts of CH_4 from the CPD to explain their compositional properties. Here, the only possible alternative is to assume a secondary origin for CH_4 in these two bodies (see Section 4).

3.2. Evolution of Solids Assuming $R_c > 30\ R_{Sat}$

In this section we examine the influence of the position of R_c on the solid abundances in the CPD. The distance out to which material is accreted onto the CPD remains uncertain and could be much larger than the current radial extent of the satellite systems of the giant planets (Drazkowska & Szulagyi 2018). In order to form the building blocks of the Saturnian moons, we would ideally need to be at a position at which the abundance of dust significantly exceeds its initial abundance, based on the minimum conditions to develop streaming instability and planetesimals (Yang et al. 2017). By expanding the centrifugal radius to larger distances, we are able to inject solids nearer each species' iceline and allow for the formation and growth of solids at greater radii. As a result, the species are able to evolve in the system for longer periods of time, even reaching an equilibrium.

Figure 5 shows simulations similar to those represented in Figure 4, but for $R_c = 66\ R_{Sat}$ and $100\ R_{Sat}$, the former value corresponding to the centrifugal radius found by Machida (2009). Within $R_c = 66\ R_{Sat}$, we are unable to form and maintain solids for long periods of time. Beyond $R_c = 100\ R_{Sat}$, the abundances of CO and N_2 are too high for current observations. For the moons to form within the constraints of the estimation of the primordial composition of their building blocks, R_c would have had to be within this interval, which is also bracketed by the positions of the CH_4 clathrate and CO icelines. Within this interval, the abundances of primordial N_2 and CO dust are negligible while those of H_2O, NH_3, and CH_4 are significant, leading to a composition similar to that expected for the building blocks of Titan and Enceladus.

Interestingly, the variation of the location of the centrifugal radius R_c affects both the temperature profile of the CPD and the positions of the various icelines. Species with icelines located at distances interior to R_c (such as H_2O and NH_3 hydrate) progress inward as R_c moves outward. In contrast, species whose icelines lie outside of R_c (such as CO and N_2 pure condensates) gradually move backward. Table 2 summarizes the locations of the various icelines in Saturn's CPD as a function of the position of R_c.

4. Discussion and Conclusion

By using a classical prescription for Saturn's CPD, we have investigated the time evolution of the icelines of H_2O ice, NH_3 hydrate, CH_4 clathrate, CO, and N_2 pure condensates, as well as their impact on the formation conditions of the building blocks of Titan and Enceladus. To match their compositional data, the building blocks of both moons would have had to form in a region of the CPD located between the icelines of CO and N_2 at their outer limit, and the iceline of CH_4 clathrate as their inner limit. We find, however, that a source of dust at the location of R_c does not guarantee the replenishment of the disk in the volatiles assumed to be primordial in Titan and Enceladus.

The centrifugal radius was initially envisioned to roughly match the radial extent of the current satellite systems, with typically assumed values of $R_c \sim 20$–$30\ R_{Sat}$, so as to account for their compactness relative to the expected sizes of the CPDs (Ruskol 1982; Canup & Ward 2002, 2006). In this case, we show that only the abundance of solid water remains substantial irrespective of time because its iceline is inside the centrifugal radius R_c. Any volatile species whose iceline

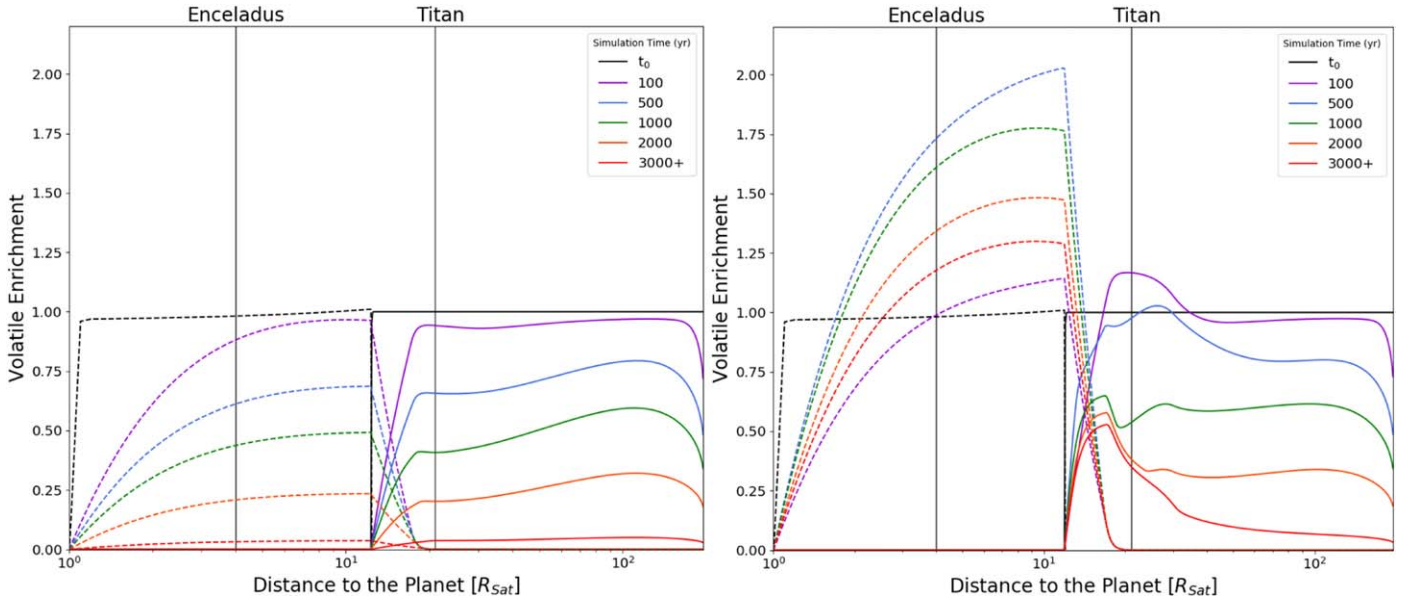

Figure 3. Evolution of water vapor (dashed lines) and ice (solid lines) in the Saturnian system over 5000 yr of evolution as a function of distance to Saturn without injection of solids (left) and with the injection of solids (right). The dust and the vapor are normalized to the initial abundance of water (H_2O/H_2) = 4.43×10^{-4}. Two things are evident: first, how quickly the particles move in the system. Second, how quickly the disk depletes: after a few thousand years, almost no dust or vapor remains if there is no source of solids.

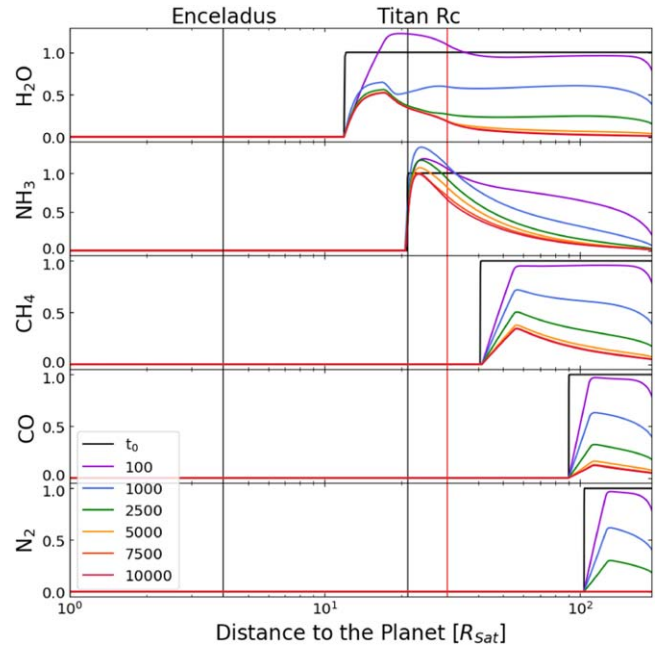

Figure 4. Evolution of H_2O, NH_3, CH_4, CO, and N_2 dust normalized to their initial abundances (see Table 1) in the Saturnian system over 10^4 yr of evolution as a function of distance to Saturn with the injection of solids. Species whose condensation radii are close to R_c (here NH_3, and H_2O to a lesser extent) retain significant abundances while the others (CH_4, CO, and N_2) deplete with time.

lies beyond depletes too rapidly for any planetesimals to form. We also performed simulations for R_c values of 66 and 100 $R_{\rm Sat}$, considering the studies made by Machida (2009) and Szulágyi (2017) regarding the structure of Saturn's CPD, and still assuming that the injection point of matter is at the location of R_c. By doing so, we are able to inject solids nearer each species' iceline and allow for the formation and growth of solids with compositions consistent with those measured in Enceladus and Titan at radii between 66 and 100 $R_{\rm Sat}$. As a result, the species are able to evolve in solid forms in the system for longer periods of time, even reaching an equilibrium, thus favoring the formation of Titan's and Enceladus's building blocks in this region of the CPD. Our results suggest that the dynamical evolution of the CPD matters little, at least to some extent. Indeed, one is able to predict the location of R_c and the formation of moon building blocks based solely on the initial pressure–temperature profile of the disk.

Our results also imply that a CPD of Saturn presenting a large centrifugal radius is also consistent with the formation of Iapetus, which is currently located at ~59 $R_{\rm Sat}$, because matter remains on longer timescales in the outer CPD. Interestingly, because the clathration temperature of Xe is higher than that of CH_4, this noble gas should be incorporated as well in the satellite's building blocks, implying that an alternative explanation is needed to explain its deficiency in Titan's atmosphere (Mousis et al. 2009a). Several post-formation scenarios have already been proposed, including the removal of Titan's noble gases by their sequestration in surface clathrates (Mousis et al. 2011), or their trapping by the haze present in the atmosphere (Jacovi & Bar-Nun 2008). One can note that the Cassini INMS did not confirm the absence of Xe shown by the Huygens GCMS because this element was beyond the mass range of the instrument (Waite et al. 2009).

The dust internal density was set to $\rho_s = 1\ {\rm g\ cm^{-3}}$ in all our calculations, corresponding to a pure icy composition in the absence of porosity. To assess the influence of the combined roles of porosity and density, we performed dust evolution simulations for ρ_s varying between 0.5 and 2 $\rm g\,cm^{-3}$. In all cases, the results are qualitatively similar to those obtained with $\rho_s = 1\ {\rm g\ cm^{-3}}$ and do not alter our conclusions.

There remain many uncertainties regarding the formation mechanism of Saturn's moon system. Some scenarios envision that all the moons accreted within the gaseous CPD of the planet (Mosqueira & Estrada 2003a, 2003b; Canup & Ward 2006). In this case, a massive moon such as Titan could have migrated inward over large distances within the CPD

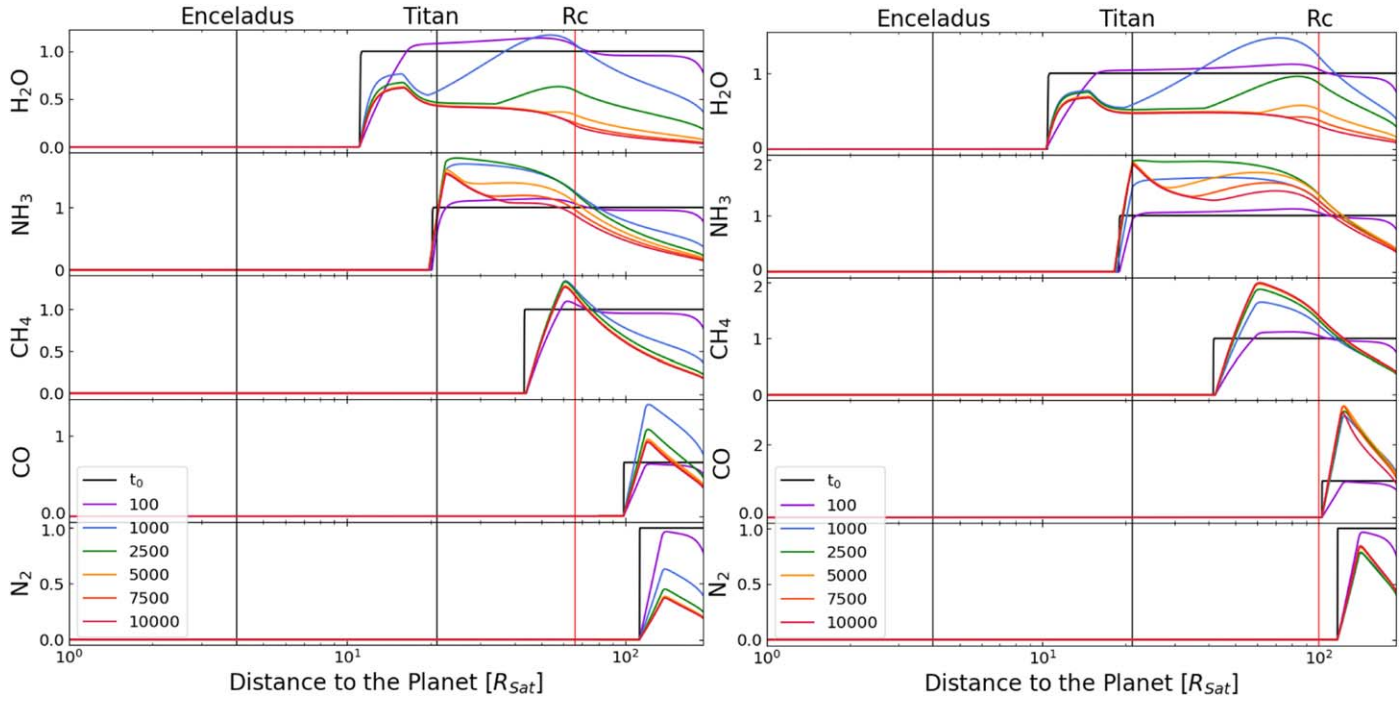

Figure 5. Evolution of H_2O, NH_3, CH_4, CO, and N_2 dust normalized to their initial abundances (see Table 1) in the Saturnian system over 10^4 yr of evolution as a function of distance to Saturn with the injection of solids at $R_c = 66\ R_{\rm Sat}$ (left) and $R_c = 100\ R_{\rm Sat}$ (right). The most consistent position of the centrifugal radius would be in between these two values. If placed beyond, the carbon monoxide solids would be highly abundant, in contrast with the inference that Titan and Enceladus accreted from CO- and N_2-depleted building blocks.

Table 2
Positions of the Icelines as a Function of the Value of R_c (in Units of $R_{\rm Sat}$)

Species	$30\ R_c = R_{\rm Sat}$	$66\ R_c = R_{\rm Sat}$	$100\ R_c = R_{\rm Sat}$
H_2O	12.0	11.2	10.5
NH_3	21.1	20.2	18.9
CH_4	40.7	43.4	41.6
CO	90.4	98.5	102.9
N_2	103.7	112.4	117.1

through tidal interaction with the gas disk (Canup & Ward 2002, 2006; Fujii & Ogihara 2020; Ronnet & Johansen 2020). Titan could have thus formed at a much larger orbital distance than its present location, in line with our findings regarding the composition of solids in the CPD. Either Titan's migration could have stopped close to its present orbit due to migration traps arising from strong thermal gradients in the CPD (Fujii & Ogihara 2020) or, alternatively, Titan could have migrated much closer to Saturn and subsequently migrated outward due to tidal interaction with the planet (Lainey et al. 2020).

In the case of Enceladus, its much smaller mass precludes a scenario involving the migration of the moon over substantial distances. However, several scenarios propose that the small and mid-sized moons of Saturn are not primordial but rather represent a second generation of satellites that would derive either from the spreading of material from Saturn's ring (Charnoz et al. 2011; Crida & Charnoz 2012; Salmon & Canup 2017) or from the disruption of a primordial system consisting of larger moons, akin to the Galilean system (Sekine & Genda 2012; Asphaug & Reufer 2013). In the latter scenario, it is possible that the primordial moons were massive enough to have migrated over substantial distances in the gaseous CPD during their accretion. If, on the other hand, Enceladus accreted from material deriving from Saturn's ring, the relevance of our results depends on the origin of the rings, which remains highly debated (see Ida 2019, for a recent review). Canup (2010) proposed that the rings could have originated from the tidal disruption of a massive (comparable to Titan) moon that would have formed in the gaseous CPD and migrated interior to the Roche radius of the planet. This scenario would remain consistent with the hypothesis of primordial methane accreted by the forming Titan and Enceladus, and is supported by the findings of the Cassini INMS instrument, which identified CH_4, CO_2, CO, N_2, H_2O, NH_3, and organics in the material of the D ring during the Grand Finale (Miller & Waite et al. 2020).

The accretion of primordial CH_4 by the moons, as proposed here, implies that the subdisk was fed low-temperature solids originating from the nebula, which were containing methane. Our model works only in the case where the inward drift of grains and particles does not exceed the metric size. However, the bulk of the solid material could have been delivered to the CPD through the capture and ablation of planetesimals on initially heliocentric orbits (Mosqueira et al. 2010; Ronnet et al. 2018; Ronnet & Johansen 2020). Small planetesimals ($r < 10$ km) could thus contribute a significant amount of material in the outer regions of the CPD. Such planetesimals would be CO- and N_2-rich and their large sizes would prevent the significant loss of ultravolatiles during their migration toward the CPD, due to their low thermal conductivity (Ronnet et al. 2017).

On the other hand, the presence of liquid water in the interiors of Titan and Enceladus (Iess et al. 2012; Waite et al. 2017) could convert CO into either CO_2 or carbonate (depending on pH) for oxidizing conditions, or reduce it to organic carbon and, eventually, CH_4 (Shock & McKinnon 1993; Glein & Waite 2018). There is also evidence from the bulk composition of comet 67P/Churyumov–Gerasimenko that

ice-poor building blocks of the outer solar system may exist (Choukroun et al. 2020). This process may also explain the depletion of CO in Titan's atmosphere relative to atmospheric N_2 and CH_4. It may also produce post-accretion N_2 from NH_3 and/or organic nitrogen (Glein et al. 2009; Neveu et al. 2017). In other words, aqueous processing of primordial volatiles in satellite oceans could also generate compositions similar to those inferred in the atmosphere of Titan or in the plumes of Enceladus. A way to constrain the origin of CH_4 in the plumes of Enceladus would to measure its D/H ratio. If the D/H ratio in CH_4 is close to the measurement of D/H in H_2O made by the INMS instrument aboard the Cassini spacecraft ($\sim 2.9 \times 10^{-4}$; Waite et al. 2009), then this methane should be the outcome of hydrothermal reactions (Mousis et al. 2009b). In contrast, a substantially lower value would be compatible with a primordial origin, i.e., methane originating from the PSN (Mousis et al. 2009b). Data on D/H in cometary methane would provide a complementary test. One would also expect a net depletion in ^{36}Ar in the plumes of Enceladus, similarly to Titan's atmosphere, if the two moons formed following our scenario. On the other hand, the plume may deplete the interior of Enceladus in volatiles. A low ^{36}Ar abundance could instead reflect a prolonged history of plume outgassing.

Our prescription of the CPD is quite rudimentary so the positions of the icelines are only indicative, since they are relative to our model, and different initial temperatures for the CPD alter the location of these lines. However, our model remains consistent with the Cassini data for a large range of R_c.

We thank two anonymous referees for their very useful remarks and comments. O.M. acknowledges support from CNES.

References

Aguichine, A., Mousis, O., Devouard, B., et al. 2020, ApJ, 901, 97
Ali-Dib, M., Mousis, O., Petit, J.-M., et al. 2014, ApJ, 785, 125
Asphaug, E., & Reufer, A. 2013, Icar, 223, 544
Atreya, S. K., Donahue, T. M., & Kuhn, W. R. 1978, Sci, 201, 611
Birnstiel, T., Klahr, H., & Ercolano, B. 2012, A&A, 539, A148
Bockelée-Morvan, D., & Biver, N. 2017, RSPTA, 375, 20160252
Bockelée-Morvan, D., Crovisier, J., Mumma, M. J., et al. 2004, in Comets II, ed. M. C. Festou et al. (Tucson, AZ: Univ. Arizona Press), 391
Canup, R. M. 2010, Natur, 468, 943
Canup, R. M., & Ward, W. R. 2002, AJ, 124, 3404
Canup, R. M., & Ward, W. R. 2006, Natur, 441, 834
Charnoz, S., Crida, A., Castillo-Rogez, J. C., et al. 2011, Icar, 216, 535
Choukroun, M., Altwegg, K., Kührt, E., et al. 2020, SSRv, 216, 44
Cilibrasi, M., Szulágyi, J., Mayer, L., et al. 2018, MNRAS, 480, 4355
Crida, A., & Charnoz, S. 2012, Sci, 338, 1196
Drazkowska, & Szulagyi, J. 2018, ApJ, 866, 142D
Fujii, Y. I., & Ogihara, M. 2020, A&A, 635, L4
Gautier, D., & Raulin, F. 1997, ESA Conf. Proc., Huygens: Science, Payload and Mission (Noordwijk: ESA), 359
Glein, C. R., Desch, S. J., & Shock, E. L. 2009, Icar, 204, 637
Glein, C. R., & Waite, J. H. 2018, Icar, 313, 79
Hersant, F., Gautier, D., & Lunine, J. I. 2004, P&SS, 52, 623
Ida, S. 2019, Sci, 364, 1028
Iess, L., Jacobson, R. A., Ducci, M., et al. 2012, Sci, 337, 457
Jacovi, R., & Bar-Nun, A. 2008, Icar, 196, 302
Lainey, V., Casajus, L. G., Fuller, J., et al. 2020, NatAs, 4, 1053
Lodders, K. 2003, ApJ, 591, 1220
Machida, M. N. 2009, MNRAS, 392, 514
Mandt, K. E., Mousis, O., Lunine, J., et al. 2014, ApJL, 788, L24
Matson, D. L., Johnson, T. V., Lunine, J. I., & Castillo-Rogez, J. C. 2007, AAS DPS Meeting, 41, 64.03
McKay, C. P., Scattergood, T. W., Pollack, J. B., et al. 1988, Natur, 332, 520
Miller, K. E., Glein, C. R., & Waite, J. H. 2019, AJ, 871, 59
Miller, K. E., Waite, J. H., Perryman, R. S., et al. 2020, Icar, 339, 113595
Mosqueira, I., & Estrada, P. R. 2003a, Icar, 163, 198
Mosqueira, I., & Estrada, P. R. 2003b, Icar, 163, 232
Mosqueira, I., Estrada, P. R., & Charnoz, S. 2010, Icar, 207, 448
Mousis, O., Alibert, Y., Hestroffer, D., et al. 2008, MNRAS, 383, 1269
Mousis, O., Lunine, J. I., Picaud, S., et al. 2011, ApJL, 740, L9
Mousis, O., Lunine, J. I., Thomas, C., et al. 2009a, ApJ, 691, 1780
Mousis, O., Lunine, J. I., Waite, J. H., et al. 2009b, ApJL, 701, L39
Mousis, O., Ronnet, T., & Lunine, J. I. 2019, ApJ, 875, 9
Mumma, M. J., & Charnley, S. B. 2011, ARA&A, 49, 471
Neveu, M., Desch, S. J., & Castillo-Rogez, J. C. 2017, GeCoA, 212, 324
Niemann, H. B., Atreya, S. K., Bauer, S. J., et al. 2005, Natur, 438, 779
Niemann, H. B., Atreya, S. K., Demick, J. E., et al. 2010, JGRE, 115, E12006
Owen, T., Mahaffy, P., Niemann, H. B., et al. 1999, Natur, 402, 269
Pepin, R. O. 1992, AREPS, 20, 389
Ronnet, T., & Johansen, A. 2020, A&A, 633, A93
Ronnet, T., Mousis, O., Lunine, J. I., & Crida, A. 2018, AJ, 155, 224
Ronnet, T., Mousis, O., & Vernazza, P. 2017, AJ, 845, 92
Ruskol, E. L. 1982, IzFZ, 6, 40
Salmon, J., & Canup, R. M. 2017, ApJ, 836, 109
Sasaki, T., Stewart, G. R., & Ida, S. 2010, ApJ, 714, 1052
Sekine, Y., & Genda, H. 2012, P&SS, 63, 133
Sekine, Y., Genda, H., Sugita, S., et al. 2011, NatGe, 4, 359
Shakura, N. I., & Sunyaev, R. A. 1973, A&A, 500, 33
Shock, E. L., & McKinnon, W. B. 1993, Icar, 106, 464
Szulágyi, J. 2017, ApJ, 842, 103
Waite, J. H., Glein, C. R., Perryman, R. S., et al. 2017, Sci, 356, 155
Waite, J. H., Lewis, W. S., Magee, B. A., et al. 2009, Natur, 460, 487
Wieler, R. 2002, RMG, 47, 21
Yang, C.-C., Johansen, A., & Carrera, D. 2017, A&A, 606, A80